Available online at www.sciencedirect.com

SciVerse ScienceDirect

Ceramics International 39 (2013) 1203–1208

CERAMICS INTERNATIONAL

www.elsevier.com/locate/ceramint

Interface evolution of the C_f/leucite composites derived from C_f/geopolymer composites

Peigang He, Dechang Jia*

Institute for Advanced Ceramics, Harbin Institute of Technology, Harbin 150080, PR China

Received 3 May 2012; received in revised form 6 July 2012; accepted 13 July 2012
Available online 27 July 2012

Abstract

In this paper, effect of heat treatment temperature on the interface structure of the carbon fiber reinforced geopolymer composites was investigated by transmission electron microscopy (TEM), selected-area diffraction (SAD) analysis and high-resolution transmission electron microscopy (HRTEM). In the composite treated at 1100 °C, carbon fiber showed a good bond with the leucite matrix and no interface reaction layer was observed, while due to the thermal mismatch between fiber and matrix, microcrack which was perpendicular to the fiber axial direction can be seen in the matrix. With increase in heat treatment temperature to 1200, 1300 and 1400 °C, interface reaction occurred and reaction layers with thickness of 50, 100 and 1000 nm, respectively, were detected. The interface layer was formed by the reaction between Si–O groups in the matrix and C element in the fiber. Especially for the sample treated at 1400 °C, serious interface reaction led to the formation of β-SiC and property of carbon fiber was greatly degraded.

Keywords: B. Interface; Carbon fiber; Leucite; Geopolymer

1. Introduction

Geopolymer materials have been developed for many years and many applications have been found for their excellent properties, like fire resistance, low density, low cost, easy processing, environmentally friendly nature and thermal resistance [1–5], and low strength and brittle fracture nature are the most serious impedances which limit their use in structural applications.

Over the past years, various kinds of reinforcements, including particulate [3,4], continuous fiber [5–9] and short fiber [10,11] reinforced geopolymer composites have been extensively investigated. Among them, continuous fiber reinforced geopolymer composites have generated a great deal of attention due to their adaptability to conventional polymer composites manufacturing techniques. Meanwhile, the high strength and modulus of the fibers can prevent catastrophic brittle failure in composites. However, due to the very weak geopolymer matrix, fiber reinforced geopolymer composites still showed low mechanical properties [3,12,13], which limit their wide applications.

Recently, many sources proved that geopolymer can be converted into advanced ceramics with high strength and stiffness by heat treatment [14–22]. In our recent research [23] we reported that after proper high temperature heat treatment, continuous carbon fiber reinforced geopolymer composite can be directly converted into carbon fiber reinforced leucite composite and mechanical properties can be greatly enhanced. The composite being treated at 1100 °C showed the highest flexural strength of 234.2 MPa, which was caused by the densified and crystallized matrix and the enhanced fiber/matrix interface bonding based on the fine-integrity of carbon fibers, and with increase in heat treatment temperature to 1200, 1300 and 1400 °C, flexural strength decreased to be 181.7, 160.3 and 54.6 MPa, respectively. Heat treatment temperature has a great effect on the interface state between leucite and carbon fiber, which played an important role in determining the whole

*Correspondence to: P.O. Box 3022, No. 2 Yikuang Street, Institute for Advanced Ceramics, HIT Science Park, Harbin Institute of Technology, Harbin 150080, PR China. Tel.: +86 451 86402040; fax: +86 451 86414291.
E-mail addresses: dcjia@hit.edu.cn, hitjiadechang@gmail.com (D. Jia)

0272-8842/$ - see front matter © 2012 Elsevier Ltd and Techna Group S.r.l. All rights reserved.
http://dx.doi.org/10.1016/j.ceramint.2012.07.045

performance of the composite. Thus, in this paper, interface structure and composition evolution caused by physical and chemical compatibility between fiber and matrix are further investigated by the TEM technique, which provides further scientific proof to support the evolution of mechanical properties of the composite with increasing treatment temperature.

2. Experimental procedures

Geopolymer resin was obtained by mixing metakaolin powder with a potassium silicate solution, as described in our previous publication [23]. The carbon fiber used in this study (Jilin Carbon Indus., China) is unidirectional continuous carbon fiber and has a diameter of 6–8 μm, and tensile strength of 2930 MPa. The composite was prepared by infiltrating geopolymer resin into the unidirectional continuous PAN-based carbon fiber preform with the help of the ultrasonic vibration treatment, and stacked one by one to get a green sample with 16 layers. To remove the pores in the green compact, degassing was applied at 80 °C for 24 h using a vacuum-bag technique. After that, the composite sample was cut into 4 parts, and each was placed at 1100, 1200, 1300 and 1400 °C, respectively, for 90 min in an argon atmosphere, to get the carbon fiber reinforced leucite composites. Composites treated at 1100, 1200, 1300 and 1400 were denoted as C-1100, C-1200, C-1300 and C-1400, respectively.

The interface microstructures were characterized by transmission electron microscopy (TEM), selected-area diffraction analysis and high-resolution transmission electron microscopy (HRTEM). Thin foil specimens taken parallel to the fiber axis were prepared by dimpling and subsequent ion-beam thinning.

3. Results and discussion

Fig. 1 shows the TEM micrographs and SAD results of C-1100. It could be observed that C_f had a good bond with the leucite matrix without obvious interfacial reaction or amorphous layer, indicating no chemical reaction between fiber and matrix occurred during composite processing. SAD result as shown in Fig. 1(b) indicated the carbon fiber was amorphous, and SAD from matrix displayed in Fig. 1(c) confirmed the formation of the crystallized tetragonal leucite, which was consistent with the XRD results in our previous publication [23].

However, microcrack in the matrix which was perpendicular to the fiber axial direction can be observed. The microcrack was mainly derived from the thermal mismatch between carbon fiber and leucite matrix during the cooling process. The average coefficient of thermal expansion (CTE) of the leucite matrix is $14.74 \times 10^{-6}\,^{\circ}C^{-1}$ from 30 °C to 1300 °C, which is higher than those of carbon fiber in both radial direction ($10 \times 10^{-6}\,^{\circ}C^{-1}$) and axial direction ($0 \times 10^{-6}\,^{\circ}C^{-1}$). Thermal mismatch would lead to the residual stress in the composite in both radial and

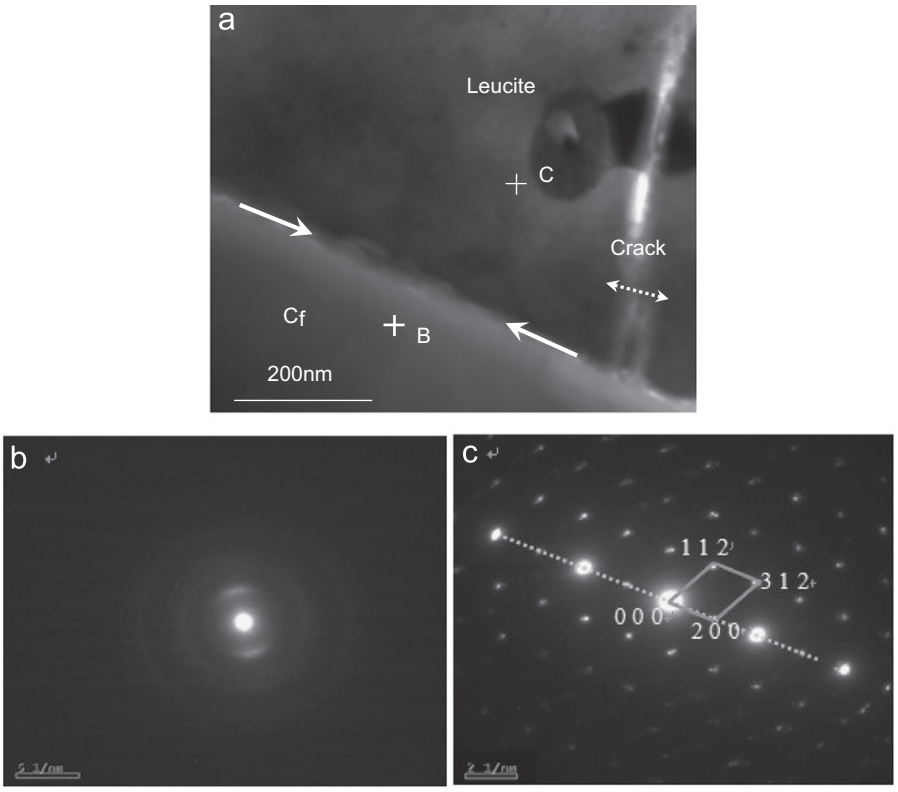

Fig. 1. Interface morphology of C-1100: (a) TEM image, (b) and (c) microdiffraction analyses of carbon fiber and matrix in area of B and C.

axial directions, which can be calculated according to formula (1) [24]:

$$\sigma = \frac{(\alpha_m - \alpha_f) \times \Delta T E_f V_f}{V_f \times \left(\frac{E_f}{E_m} - 1\right) + 1} \quad (1)$$

where α_m, $\alpha_{f.a}$ and $\alpha_{f.r}$ are the CTE of the leucite matrix, carbon fiber in axial and radial direction, of 14.74×10^{-6} °C^{-1}, 0, and 10×10^{-6} °C^{-1}, respectively; E_m and E_f are the modulus of leucite matrix and carbon fiber, of 65 GPa and 220 GPa; and ΔT is the temperature range from 1100 to 1400 °C. The calculated results are shown in Table 1. In radial direction, the thermal mismatch could result in the residual compressive stress between fiber and matrix, which would increase the bonding strength between them during cooling and was beneficial to the property improvement of the composite. Therefore, in the radial direction, the thermal expansion mismatch between fiber and matrix was acceptable, while in axial direction, the thermal mismatch would result in the significant tensile strength in leucite matrix. As shown in Table 1, for C-1100, the residual tensile strength was 557.5 MPa. It was much higher than that of the leucite matrix (about 70 MP), thus led to the transverse microcrack in the matrix. The microcrack in the matrix would undoubtedly decrease the crack tolerance of the leucite matrix and was detrimental to the mechanical properties of the composites. Cs^+ partial-substitution for the K^+ has been proved to be an efficient method to decrease the coefficient of thermal expansion of the leucite matrix [25] and thus increase the thermal compatibility between matrix and the carbon fiber and enhance the properties of the composite, which will be carried out in a later investigation.

Interface morphologies of the C-1200, C-1300 and C-1400 are shown in Figs. 2–4, respectively. It can be observed the interface reaction layers with thickness of ~50 nm and ~100 nm were formed for C-1200 and C-1300, respectively, implying the interface bonding transformed from the initial physical bonding for C-1100 into chemical bonding for C-1200 and C-1300. Furthermore, when heat treatment temperature was increased to 1400 °C, as shown in Fig. 4, the thickness of the reaction layer increased sharply to be 1000 nm for C-1400, indicating serious interface reaction occurred and property of carbon fiber was substantially degraded. SAD pattern of the area B (Fig. 4(b)) in the reaction layer was composed of the amorphous carbon fiber (the central diffraction spot and crescent spots in both upper and lower sides) and β-SiC (the circulated diffraction spots). As shown in Fig. 5(a) and (b), HREM image of area B proved the typical stack faults within the reaction layer structure, and FFT transformed image further confirmed the formation of the β-SiC.

Table 1
Thermal residual stress in the composites during cooling process.

ΔT (°C)	1100	1200	1300	1400
σ_a (MPa)	557.5	608.2	658.9	709.6
σ_r (MPa)	195.5	213.3	231.0	248.8

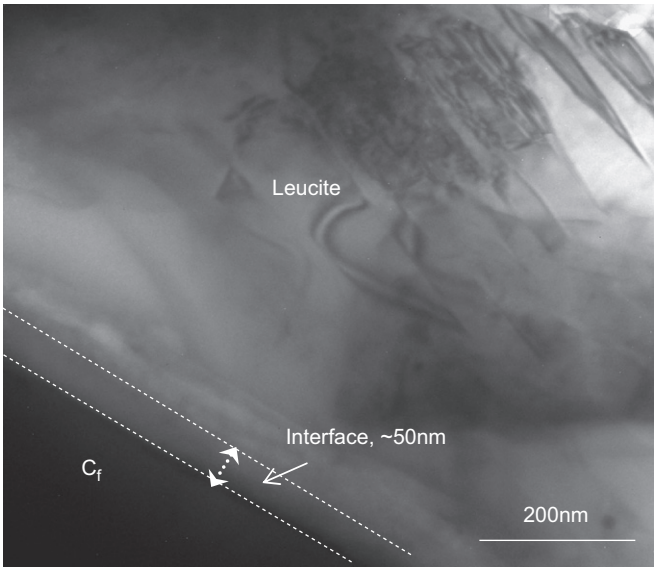

Fig. 2. Interface morphology of C-1200.

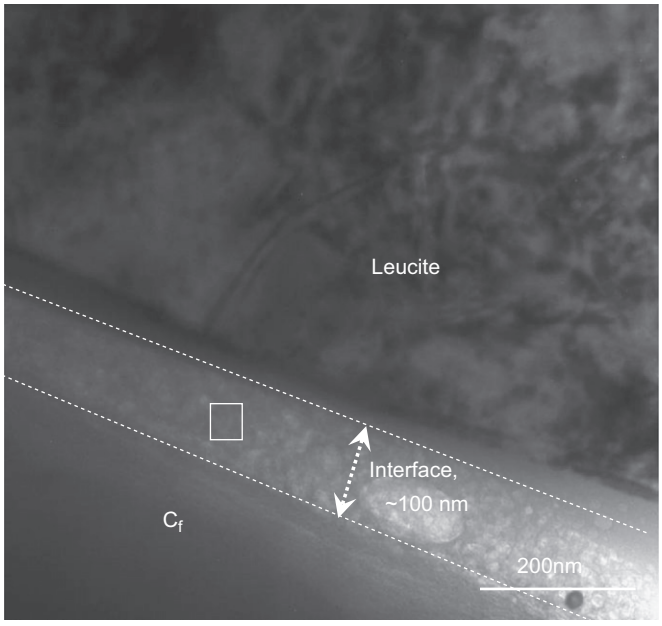

Fig. 3. Interface morphology of C-1300.

The element distributions in the box region in Figs. 2–4 are shown in Fig. 6. Si, Al and K atoms were detected in the interfacial area, indicating the inter-diffusions of these atoms between matrix and fiber, and with increasing heat treatment temperature, the extent of the atom diffusion increased gradually.

Fig. 7 shows the interface at the ends of fiber in C-1100 and C-1400. Fig. 7(a) shows that long fiber pull-out dominated the fracture surface of C-1100 and high-magnification SEM image (Fig. 7(b)) shows that the fibers all maintained fine-integrity, so interface reaction did not occur at 1100 °C and a relatively

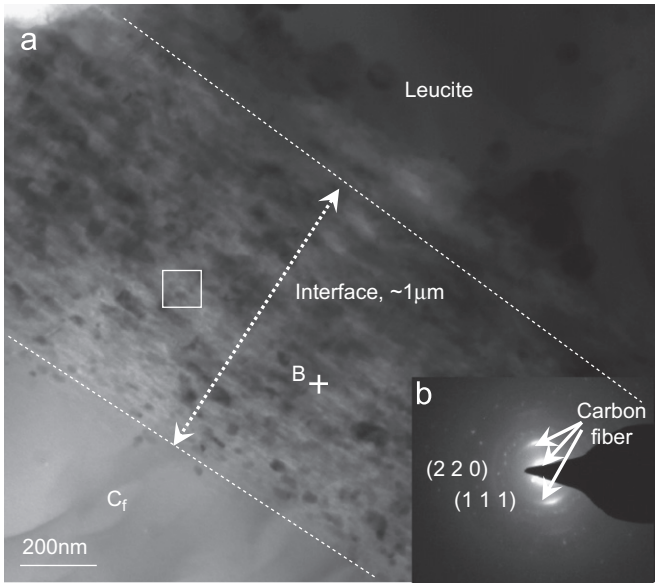

Fig. 4. Interface morphology of C-1400: (a) TEM image, (b) microdiffraction analysis of area B.

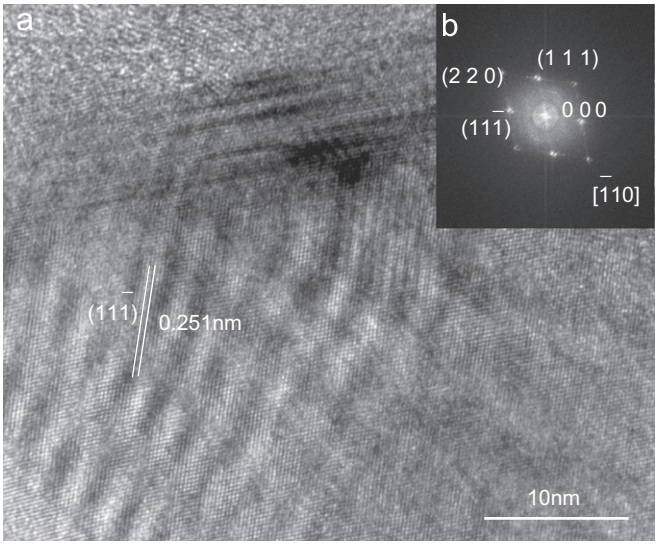

Fig. 5. HRTEM micrographs of area B in Fig. 4: (a) HRTEM image and (b) FFT transformed image.

weak C_f/matrix interfacial bonding was achieved. However, for C-1400 fracture surface was much more flat and few fibers pull-out could be observed than C-1100, as shown in Fig. 7(c). Meanwhile, high-magnification SEM image (Fig. 7(d)) showed the formation of an interface reaction layer of about 1 μm in thickness indicating the fiber was highly corroded, which was in accordance with the TEM results in Fig. 4.

Together with the TG and XRD results in our previous results [23] and total vapor pressure of interfacial reaction of Si–C–O system as a function of temperature [26], the interface layer was generated by the reaction between Si–O groups in the matrix and C element in the fiber, leading to the formation of SiC and CO, as shown in reaction (1):

$$SiO_2 + C \rightarrow SiC + CO(g) \quad (1)$$

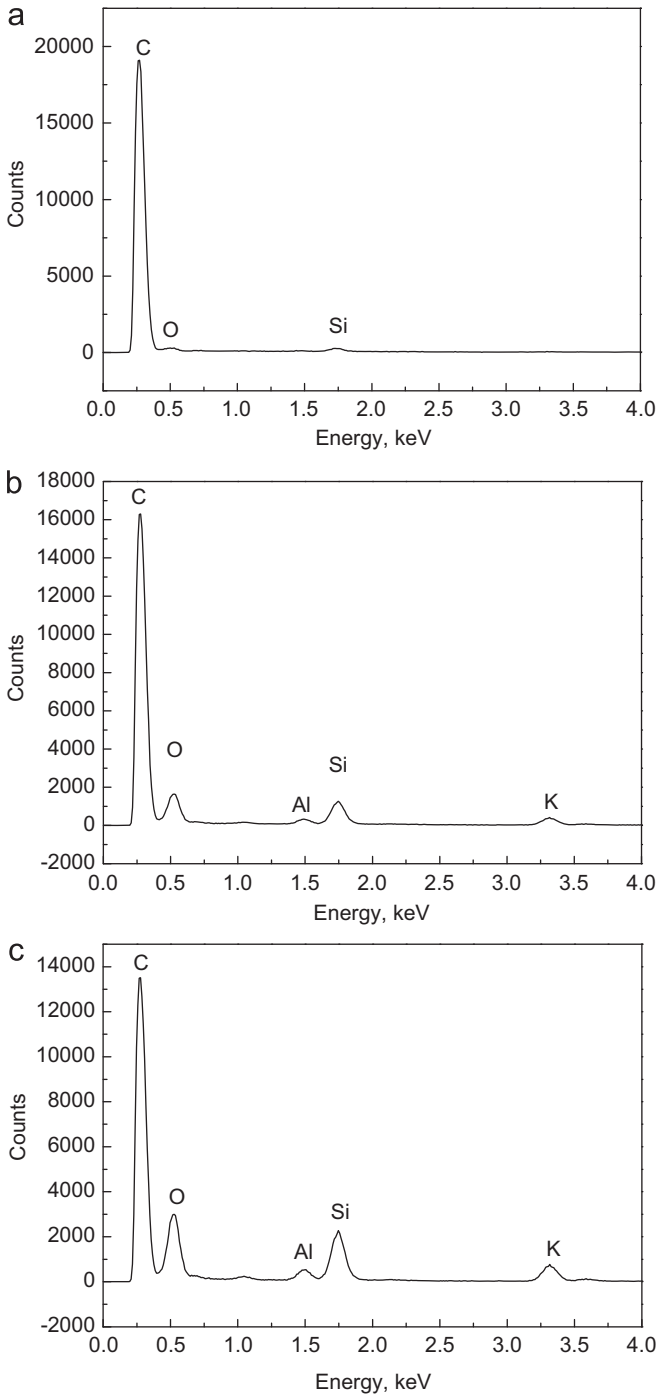

Fig. 6. Element distributions in the interface region: (a) C-1200, (b) C-1300, (c) C-1400.

According to the standard formation Gibbs free energy of each reaction shown in Table 2, the Gibbs free energy for the reaction (1), ΔG°, can be calculated by formula (2):

$$\Delta G^\circ = 605250 - 339.61T \quad (2)$$

When ΔG° is lower than 0, the reaction between Si–O and C can occur, so the theoretical lowest reaction temperature should be 1782.2K (1509.2 °C) according to formula (2). However, evident reaction layer can be

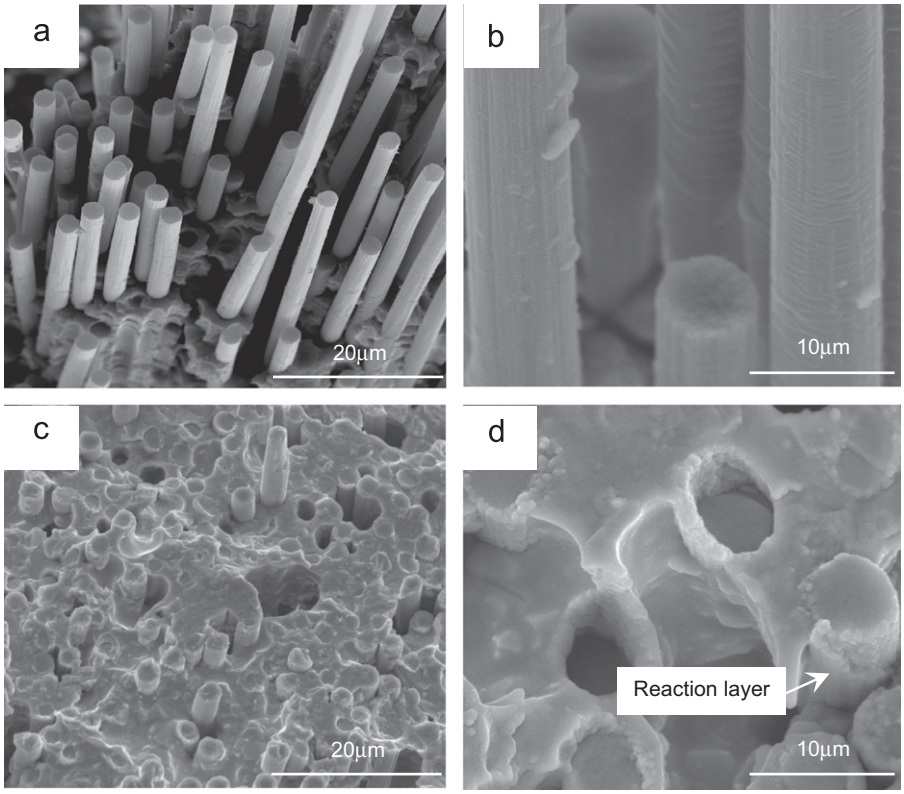

Fig. 7. Interface at the ends of fiber in (a)–(b) C-1100 and (c)–(d) C-1400.

Table 2
The reactions and standard Gibbs free energy.

Reaction	Standard Gibbs free energy ($J\ mol^{-1}$)
(1) $C_{(s)}+0.5O_{2(g)}\rightarrow CO_{(g)}$	$-114400-85.77T$
(2) $Si_{(s)}+C_{(s)}\rightarrow SiC_{(s)}$	$-73050+7.66T$
(3) $Si_{(s)}+O_{2(g)}\rightarrow SiO_{2(s)}$	$-907100+175.73T$

observed in sample C-1200, and thermogravimetric analysis proved the initial reacting temperature was as low as 1170 °C [23], which was much lower than the theoretical result and that in the C_f/SiO_2 system [26]. It might be attributed to the existence of K^+ in the matrix. Because the bond energy of K–O is much lower than that of the Si–O [27], the oxygen which is connected with the K^+ can be easily captured by the Si^{4+} at high temperature, and thus the bridge oxygen bonds to the Si^{4+} in the Si–O groups were disconnected. Therefore, the frame polystructure of the Si–O groups was decomposed to be a variety of oligomers, which results in the decreased viscosity of the leucite matrix at high temperature as compared with the pure SiO_2 matrix [26]. Although the low viscosity was helpful to the densification of the composite, it was also associated with the much more accelerated atom movement, which made the interface reaction occur at low temperature.

The formation of the interface reaction layer would greatly enhance the interface bonding strength, and then facilitate the load transferring from matrix to fiber and improve the reinforcing role of the carbon fiber. However, interface reaction will also result in the property degradation of carbon fiber, which would decrease the mechanical properties of the composites. With increasing heat treatment temperature from 1100 to 1300 °C, mechanical properties of the composites tended to decrease gradually [23], implying the negotiate effect of the interface reaction was more pronounced than its positive effect. Especially for C-1400, carbon fiber was seriously corroded and mechanical properties of the composite were dramatically lowered.

4. Conclusion

With increasing heat treatment temperature, the interface states of the carbon fiber reinforced leucite composites transformed from the physical bonding at 1100 °C to chemical bonding at temperature range of 1200–1400 °C caused by interface reaction. Interface reaction would result in the fiber degradation and thus was detrimental to the properties of the composites, so the heat treatment temperature of the composites should not exceed the onset temperature of interface reaction. Thermal mismatch in radial direction was beneficial to the property improvement of the composite, while that in axial direction resulted in microcrack in matrix which was perpendicular to fiber axial direction. Therefore, efficient way to improve

the physical and chemical compatibility between fiber and matrix should be further investigated.

Acknowledgments

This work was supported by the Program for New-Century Excellent Talents in University (NCET, Grant no. NCET-04-0327), the Program of Excellent Team in Harbin Institute of Technology, and the Science Fund for Distinguished Young Scholars of Heilongjiang Province. We are very grateful to Professor Liu Kedong of the Department of English Language at Harbin Institute of Technology for his assistance in proofreading.

References

[1] J. Davidovits, Geopolymer—inorganic polymeric new materials, Journal of Thermal Analysis 37 (8) (1991) 1633–1656.
[2] J. Davidovits, 30 Years of Successes and Failures in Geopolymer Applications, Geopolymer Conference, Melbourne, Australia, 2002.
[3] J. Davidovits, M. Davidovics, Geopolymer: ultra-high temperature tooling material for the manufacture of advanced composites, SAMPE 36 (2) (1991) 1939–1949.
[4] V.F.F. Barbosa, K.J.D. MacKenzie, Thermal behaviour of inorganic geopolymers and composites derived from sodium polysialate, Materials Research Bulletin 38 (2) (2003) 319–331.
[5] C.G. Papakonstantinou, P.N. Balaguru, R.E. Lyon, Comparative study of high temperature composites, Composites Part B 32 (8) (2001) 637–649.
[6] R.E. Lyon, P.N. Balaguru, A. Foden, U. Sorathia, J. Davidovits, M. Davidovics, Fire-resistant aluminosilicate composites, Fire and Materials 21 (4) (1997) 67–73.
[7] Q. Zhao, B. Nair, T. Rahimian, P.N. Balaguru, Novel geopolymer based composites with enhanced ductility, Journal of Materials Science 42 (9) (2007) 3131–3137.
[8] P.N. Balaguru, C. Defazio, M.D. Arafa, and B. Nair, Functional Geopolymer Composites for Structural Ceramic Application, Ceram–RU9163, 〈http://cait.rutgers.edu/files/Ceram–RU9163.pdf〉.
[9] B.G. Nair, Q. Zhao, R.F. Cooper, Geopolymer matrices with improved hydrothermal corrosion resistance for high–-temperature applications, Journal of Materials Science 42 (9) (2007) 3083–3091.
[10] Y.S. Zhang, W. Sun, Z. Li, X. Zhou, Geopolymer extruded composites with incorporated fly ash and polyvinyl alcohol short fiber, ACI Materials Journal 106 (1) (2009) 3–10.
[11] T.S. Lin, D.C. Jia, P.G. He, M.R. Wang, D.F. Liang, Effects of fiber length on mechanical properties and fracture behavior of short carbon fiber reinforced geopolymer matrix composites, Materials Science and Engineering A 497 (1–2) (2008) 181–185.
[12] W.M. Kriven, J. Bell, M. Gordon, Microstructure and Microchemistry of Fully-Reacted Geopolymers and Geopolymer Matrix Composites, in: N.P. Bansal, J.P. Singh, W.M. Kriven, H. Schneider (Eds.), in Ceramic Transactions, Advances in Ceramic Matrix Composites, vol. 153, The American Ceramic Society, Westerville, OH, 2003, pp. 227–250.
[13] N. Davidovits, M. Davidovics, J. Davidovits, Ceramic-Ceramic Composite Material and Production Method, U.S. Patent 4888311, 1988.
[14] V.F.F. Barbosa, K.J.D. MacKenzie, Synthesis and thermal behaviour of potassium sialate geopolymers, Materials Letters 57 (9–10) (2003) 1477–1482.
[15] V.F.F. Barbosa, K.J.D. MacKenzie, Thermal behaviour of inorganic geopolymers and composites derived from sodium polysialate, Materials Research Bulletin 38 (2) (2003) 319–331.
[16] J.L. Bell, P.E. Driemeyer, W.M. Kriven, Formation of ceramics from metakaolin-based geopolymers: Part I—Cs-based geopolymer, Journal of the American Ceramic Society 92 (1) (2009) 1–8.
[17] J.L. Bell, P.E. Driemeyer, W.M. Kriven, Formation of ceramics from metakaolin-based geopolymers. Part II: K-based geopolymer, Journal of the American Ceramic Society 92 (3) (2009) 607–615.
[18] P. Duxson, G.C. Lukey, Physical evolution of Na-geopolymer derived from metakaolin up to 1000 °C, Journal of Materials Science 42 (9) (2007) 3044–3054.
[19] P. Duxson, G.C. Lukey, S.J. Jannie, V. Deventer, The thermal evolution of metakaolin geopolymers: Part 2—phase stability and structural development, Journal of Non-Crystalline Solids 353 (22–23) (2007) 2186–2200.
[20] A. Riessen, Thermo-mechanical and microstructural characterisation of sodium-poly(sialate-siloxo)(Na-PSS) geopolymers, Journal of Materials Science 42 (9) (2007) 3117–3123.
[21] P. He, D. Jia, T. Lin, M. Wang, Y. Zhou, Thermal evolution and crystallization kinetics of potassium-based geopolymer, Ceramics International 37 (2011) 59–63.
[22] N. Xie, J.L. Bell, W.M. Kriven, Fabrication of structural leucite glass-ceramics from potassium-based geopolymer precursors, Journal of the American Ceramic Society 93 (9) (2010) 2644–2649.
[23] P. He, D. Jia, T. Lin, M. Wang, Y. Zhou, Effects of high-temperature heat treatment on the mechanical properties of unidirectional carbon fiber reinforced geopolymer composites, Ceramics International 36 (2010) 1447–1453.
[24] R.J. Kerans, T.A. Parthasarathy, Theoretical analysis of the fiber pullout and push out test, Journal of the American Ceramic Society 74 (1991) 1585–1589.
[25] P. He, D. Jia, T. Lin, M. Wang, Y. Zhou, Effect of cesium substitution on the thermal evolution and ceramics formation of potassium-based geopolymer, Ceramics International 36 (2010) 2395–2400.
[26] G.W. Wen, Microstructure and Properties of Fused Silica Composites, Ph.D. Thesis, Harbin Institute of Technology, China, 1996.
[27] Y. Zhou, Physics and Chemistry of Inorganic Materials, Wuhan University of Technology, China, 1994.